Theor Chim Acta (1992) 83: 123–139

Theoretica Chimica Acta

Localized molecular orbitals in CI calculations of organic molecules*

Thomas Neuheuser, Malte von Arnim, and Sigrid D. Peyerimhoff
Institut für Physikalische und Theoretische Chemie, Universität Bonn, Wegelerstraße 12, W-5300 Bonn 1, Federal Republic of Germany

Received May 10, 1991/Accepted October 2, 1991

Summary. Configuration Interaction (CI) calculations are carried out for bond-breaking processes by employing localized molecular orbitals (LMO). It is found that the advantage of this choice relative to the use of canonical orbitals is two-fold: First, the convergence of the truncated CI is speeded up by employing LMO; secondly, since the LMO are localized in certain regions of the molecular system one can divide the LMO in two sets, one which is important for the description of the process under consideration and the other which describes the molecular part not directly involved in the process ("spectator group"). It is found to be sufficient to correlate only the "local active region" of the molecule, and this procedure leads to a much shorter CI expansion without loss of accuracy in describing the chemical process. The CH_3 group has been used as "spectator group" and the dissociation into radicals $CH_3X \rightarrow CH_3 + X$ and $CH_3CH_2X \rightarrow CH_3CH_2 + X$ with $X = H, F, NH_3^+$ as well as the charge transfer reaction $CH_3\text{–}X^+ \rightarrow CH_3^+ + X$ and $CH_3CH_2\text{–}X^+ \rightarrow CH_3CH_2^+ + X$ with $X = N_2$ and NH_3 has been studied. For both type of radical reactions the CH_3 bonds need not be included in the local active region, while in the charge-transfer process the CH_3 can only be considered a spectator group if it is not connected directly to the separating group.

Key words: CI calculations – LMO – Bond-breaking processes

1. Introduction

In full configuration interaction (CI) calculations the choice of the one-particle basis functions is immaterial because the various sets are related by a unitary transformation. In truncated CI schemes, on the other hand, the choice of the molecular basis set can be quite important in order to insure fast convergence [1–4]. A number of orbitals are generally in use, such as canonical SCF orbitals (of various electronic states), natural orbitals in various modifications [4, 5],

* Dedicated to Prof. Klaus Ruedenberg on the occasion of his 70th birthday

CASSCF orbitals [6] and others. In the present study we will employ localized molecular orbitals (LMO).

The motivation for this choice arises from the following consideration: In a number of instances one is interested in the description of predominantly local processes within a molecule, such as bond-breaking, adsorption to a surface or local excitation. In such cases it is conceivable that only that portion of the molecule, in which the process occurs ("local active region"), must be represented by properly correlated wavefunctions while the remaining part of the system ("spectator group") may be treated in a less rigorous manner. Since the canonical orbitals are generally delocalized over the entire molecule, they are not especially adequate for the description of local processes. On the other hand, localized MO are very feasible for such a treatment, so that the LMO of the local active region are employed in the configuration interaction procedure, while those LMO describing in the main the spectator group keep the same occupation in all configurations. It is also clear that the importance of this concept of differentiating between various parts of a molecule becomes more and more important as the size of the molecule increases.

This basis concept of a "local active region" has for example been employed to calculate the dissociation energy of nitro compounds. In particular, the dissociation of nitrobenzene into a phenyl radical plus NO_2 has been studied [7] whereby the local active region included the NO_2, the C–N bond plus the neighboring two CC bonds of the benzene ring. Similarly the reaction between oxetane and protonated oxetane has been studied in such a framework as a model case for a cationic catalytic polymerization [8]. The dissociation of nitromethane in a crystal into a methyl radical plus NO_2 has also been studied by describing the dissociating molecule via correlated wavefunctions while the remaining crystal was simulated in a more global (SCF and multipole expansion) manner without taking account of electron correlation [9, 10].

A central question in such a concept is how the partitioning into "local active region" and "spectator group" is achieved. In particular there is the question how far away can the spectator group be from the active region without any loss of accuracy in the calculations due to this approach, in comparison with the all-electron or all-valence-electron calculations.

A typical "spectator group" in organic reactions is the methyl group. In order to investigate the various situations, in which this CH_3 group can be described without accounting for electron correlation, it is necessary to consider borderline cases, in which this group has quite variable influence on the process under consideration. Hence in the present paper we considered the simple radical reactions:

$$CH_3\text{–}X \rightarrow CH_3\cdot + \cdot X$$

$$CH_3\text{–}CH_2\text{–}X \rightarrow CH_3\text{–}CH_2\cdot + \cdot X$$

with X = H, F, and NH_3^+, whereby the substituents were chosen such that they have different polarity. In addition, the more complicated reactions involving a charge transfer from X to CH_3:

$$CH_3\text{–}X^+ \rightarrow CH_3^+ + X$$

$$CH_3CH_2\text{–}X^+ \rightarrow CH_3\text{–}CH_2^+ + X$$

with $X = N_2$ and NH_3 will also be studied.

The aim thereby is to employ LMO in a CI treatment and find out which of the LMO have to be included in the CI wavefunctions in order to describe the above bond-breaking process, and which can be considered to possess fixed occupation.

2. Technical details

The AO basis sets employed for carbon, nitrogen and fluorine atoms in the various calculations are the (9*s*5*p*) Gaussian sets by Huzinaga in the [4*s*2*p*] contraction suggested by Dunning [11]. One *d* function has been added with exponents $d(C) = 0.6$, $d(N) = 0.864$ and $d(F) = 1.5$. The hydrogens are described by a Gaussian expansion of four *s* functions in a [2*s*] contraction, also given by Dunning [11].

The first step in the computational procedure is the SCF calculation. For $CH_3CH_2N_2^+$ additional complete-active-space (CAS) calculations [12] have been carried out and are described in connection with the results. The *d* functions are used with five (and not the cartesian six) components. The coefficient vectors for the 1*s* orbitals of C, N and F are taken directly from atomic SCF calculations. In the SCF or the CASSCF calculations for the molecule these orbitals ("core orbitals") are simply orthonormalized but not optimized any more. This is justifiable because the K-core function (not its canonical energy) remains to a large extent the same when introduced into the molecular surrounding. This fact is also used, for example, in calculations in which the 1*s* functions of first-row atoms are represented by an effective core potential [13, 14]; this substitution does not cause any loss of accuracy in the description of relative energies or other properties which do not directly depend on the K shell functions.

The localization of the canonical SCF orbitals was undertaken for all valence orbitals according to the procedure of Foster and Boys [15]. By valence orbitals we mean all orbitals with the exception of the above mentioned 1*s* core orbitals and their complement with the highest orbital energy (and largest orbital exponents), one corresponding to each 1*s* orbital. The latter differ from the 1*s* core only by radial nodes; they can serve to correlate the 1*s* core orbitals which is not necessary in the present context, however. Hence both sets of valence orbitals, the occupied and the virtuals, are localized (separately from each other). The orbitals from the CASSCF were localized in the analogous manner as the SCF orbitals with the restriction that the active orbitals are not further localized. This was possible because the active orbitals were automatically localized (see Sect. 4.1). In the localization procedure only SCF or CASSCF orbitals within the same irreducible representation were mixed, however, so that the symmetry properties (plane of symmetry in this case), which are important for the CI calculation, could be maintained. The localization of MO within a given symmetry did not cause any difficulties.

The CI calculations were of the standard multi-reference (MRD-CI) type with configuration selection according to a threshold criterium and extrapolation of the energy to zero threshold [3, 17]; the full CI energy was also estimated by a modified Davidson correction [18]. The energy obtained from the secular equation corresponding to the selected configurations with selection threshold T will be referred to as $E(T)$, the energy extrapolated to zero selection threshold corresponding to the full generated MRD-CI space will be denoted by $E_{\text{MRD-CI}}$ and the estimated full CI energy as $E_{\text{est.FCI}}$.

The CI calculations are undertaken in two ways: (1) standard CI procedures employing all valence MO, referred to as valence configuration interaction (VCI), in which either canonical MO, referred to as VCI/MO, or localized MO, denoted by VCI/LMO, were employed. (2) "Local active region" CI calculations referred to as LCI; these do not correlate the electrons in the methyl group and employ only the localized orbitals (LCI/LMO). Calculations of the LCI/MO type are generally not possible because the canonical MO cannot be divided into those of the methyl group and those of the local active region. Various additional computations, in which excitations into the virtual LMO of the methyl group are also allowed, are carried out for comparison with those treatments, which do not include any LMO of the CH_3 group. The number of reference configurations ("mains") used in the CI calculations is indicated as follows: VCI(n) means a valence CI calculation with n reference configurations (LCI(n) is defined analogously). Adding the type of orbital optimization we use for example VCI(16)/CAS LMO as an abbreviation for a valence CI calculation with localized CAS orbitals and 16 reference configurations. In the case of CI calculations without configuration selection (selection threshold $T = 0$) and one reference configuration the result is the same for SCF MO and SCF LMO (due to invariance of the CI space), so we did not indicate which type of SCF orbitals is used (Tables 3, 4, 5).

Finally, the geometries considered for $CH_3N_2^+$ and $CH_3CH_2N_2^+$ result from an optimization employing GAUSSIAN86 [19] at the HF/6-31G level; for all other systems geometries based on MNDO [20] calculations are employed.

3. Calculations on the methyldiazonium ion $CH_3N_2^+$

Computations are undertaken for $CH_3N_2^+$ in its calculated equilibrium geometry (Fig. 1) and for the supermolecule at $R_{CN} = 50$ Å representing $CH_3^+ + N_2$. In the planar CH_3^+ fragment $R_{CH} = 1.077$ Å, in N_2 the bond length $R_{NN} = 1.089$ Å. In the calculated geometry of $CH_3N_2^+$ two points are worth mentioning: First, the value of 1.513 Å is relatively large for a CN single bond, in particular since the CN bond in methyl-amin is observed to be only 1.47 Å [21]. It is conceivable that the large value is a consequence of neglecting electron correlation in the geometry optimization, since Ford [22] obtains a reduction from 1.510 Å (HF/6-31G*) to 1.46 Å upon partial consideration of electron correlation in the MP2/6-31G* procedure. Secondly, the NN distance in $CH_3N_2^+$ has the same length as in N_2. This can be explained from qualitative reasons considering the moelcular orbitals: In the canonical MO picture the CN bond results from mixing of a nonoccupied carbon orbital with the occupied $2\sigma_u$ (NN antibonding)

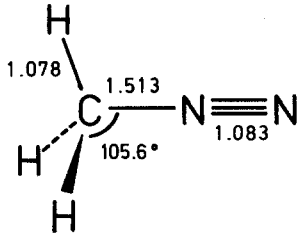

Fig. 1. Calculated equilibrium structure of $CH_3N_2^+$ (bond lengths in Å)

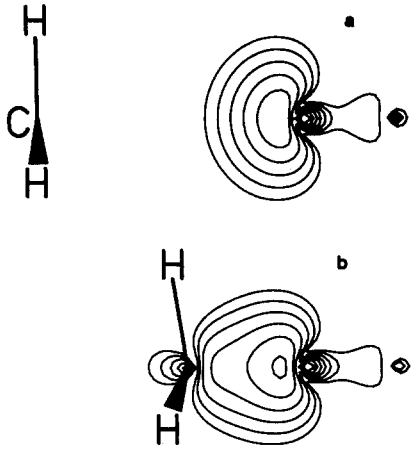

Fig. 2. Charge density contours of the N_2 lone pair (**a**) in the separated fragments $[CH_3 + N_2]^+$ and (**b**) in the molecular $[CH_3N_2]^+$ environment

as well as the $3\sigma_g$ (NN bonding) orbital [23] so that the net effect of the carbon with respect to the N_2 bond is zero. In the localized orbital picture the CN bond is formed by interaction of the empty carbon orbitals with a lone pair on N_2. The charge density of this LMO is plotted in Fig. 2 for the separated and the compound species, and it is seen that this CN bonding orbital has very little effect on the NN bond.

Details of the various MRD-CI calculations carried out for the two geometries are given in Table 1. Given are the energies $E(T)$ at the selection threshold of $T = 5\ \mu H$, the energy $E_{MRD\text{-}CI}$ extrapolated to zero threshold and the estimated full CI energy. In addition, the total number of generated configurations (or rather symmetry adapted functions SAF) as well as the number directly selected for the secular equation resulting in $E(T)$, are listed. The last column contains the sum

Table 1. $CH_3N_2^+$: Influence of the orbital basis on the convergence of the CI expansion

Method	$E(T)$	$E_{MRD\text{-}CI}$	$E_{est.FCI}$	c^2	SAF total	SAF selected	Energy sum
			$CH_3N_2^+$				
VCI(6)/SCF MO	−0.62578	−0.64385	−0.68053	0.899	273786	7360	0.02226
VCI(4)/SCF LMO	−0.61605	−0.63210	−0.66807	0.903	257803	3443	0.01171
LCI(4)/SCF LMO	−0.51505	−0.52500	−0.54394	0.928	83967	1893	0.00474
LCI(4)[a]/SCF LMO	−0.51399	−0.52262	−0.54124	0.929	54279	1837	0.00414
			$CH_3^+ + N_2$				
VCI(8)/SCF MO	−0.57893	−0.58744	−0.61499	0.912	321899	1824	0.00776
VCI(5)/SCF LMO	−0.56383	−0.56923	−0.60325	0.902	309744	2589	0.00326
LCI(4)/SCF LMO	−0.47344	−0.47745	−0.49712	0.925	99568	2080	0.00215
LCI(4)[a]/SCF LMO	−0.47344	−0.47745	−0.49712	0.925	64171	2058	0.00215

SCF energy of $CH_3N_2^+$: −148.23925 a.u.
SCF energy of $CH_3^+ + N_2$: −148.19447 a.u.
VCI(n) = valence CI with n Mains (16 electrons correlated)
LCI(n) = "local active region" CI with n Mains (10 electrons correlated)
Energies in a.u.; $E(T)$, $E_{MRD\text{-}CI}$ and $E_{est.FCI}$ relative to −148 a.u.
Selection threshold $T = 5\ \mu H$
[a] Virtual CH_3-LMO not included in the CI

of the energy contributions of all SAF not selected, evaluated for each SAF individually relative to the energy of the reference configurations. All configurations which occurred in a preliminary 1-reference calculation with a weight larger than $c^2 = 0.002$ were included in the reference set; the weight of the reference configurations in the final CI expansion was in all cases 90% or higher. In the VCI calculations all 16 valence electrons are correlated. In the LCI calculation only 10 electrons are correlated, namely the electrons of the CN bond, of the NN triple bond plus the *N* lone pair electrons; the six electrons of the CH bonds are not included in the LCI. The virtual LMO are treated in two different ways. In the first calculation the virtual LMO of the methyl group are included in the LCI and in the second calculation they are not allowed for variable occupation (short-hand notation: "virt. CH_3-LMO not in CI").

It is seen from Table 1 that the VCI/MO results give the lowest total energy. But this is immaterial since the goal is not to obtain as much as possible of the total correlation energy, but rather to include that part of the correlation energy which is important for the process under consideration. If we consider first the equilibrium geometry, we find that employing localized orbitals rather than canonical orbitals in the valence CI, results naturally in almost the same number of total SAF (slightly different because in one case six reference configurations and in the other only four are of importance, i.e. those configurations which appear in a preliminary CI with a weight of $c^2 > 0.002$), but the number of selected species, which have to be treated directly in the CI, is in the VCI/LMO treatment only about half of that of the standard VCI/MO. This simply means that the truncated CI expansion employing LMO is more compact within the MRD-CI space than if MO are used, a finding which is also reflected in the energy sum of the generated but not explicitly selected SAF. For the separated fragments the VCI with LMO includes also a larger portion of the more strongly interacting SAF directly in the secular equation (energy sum of the unselected only 0.00326), but the VCI/LMO calculation is somewhat more expensive than that of VCI/MO. The reason for the larger number of selected SAF in the VCI/LMO treatment is the σ-π mixing of LMO in N_2; in order to account for the important π-π^* type, excitations, also σ-σ^* type contributions must be considered in the LMO picture.

If we continue to compare only canonical and localized orbitals in the same kind of VCI, we find that the dissociation energy (Table 2) is almost the same in both treatments at the estimated full CI level. This value is comparable to the

Table 2. Dissociation energy of $CH_3N_2^+$

Method	$\Delta E(T)$ (eV)	$\Delta E_{\text{MRD-CI}}$ (eV)	$\Delta E_{\text{est.FCI}}$ (eV)
VCI/SCF MO	1.28	1.54	1.78
VCI/SCF LMO	1.42	1.71	1.76
LCI/SCF LMO	1.13	1.29	1.27
LCI[a]/SCF LMO	1.10	1.23	1.20

The SCF value is 1.22 eV
VCI = valence CI (16 electrons correlated)
LCI = "local active region" CI (10 electrons correlated)
Selection threshold $T = 5\ \mu H$
[a] virtual CH_3-LMO not included in the CI

1.84 eV obtained by Ford [22] in a calculation at the MP4(SDQ)/6-31G* level; perturbation theory is applicable in this case since the SCF configuration is dominant ($c^2 \approx 0.9$) in the CI expansion. At the same time it is obvious that the VCI/LMO yields the more reliable results at the intermediate levels of treatment, i.e. $E(T)$ and E_{MRDCI}, simply because the contribution of the unselected SAF (energy sum in Table 1) is smaller in the VCI/LMO than in the VCI/MO treatment.

If one considers now the LCI with VCI one observes considerable advantages for the technical part of the calculations (Table 1) in the LCI, but certainly disadvantages as far as the chemical part (Table 2) is concerned.

As expected, the total number of SAF is drastically reduced in the LCI (because only 10 instead of 16 electrons are correlated), the selected MRD-CI subspaces are also smaller, in particular for the molecular state. Likewise the energy contributions of the SAF not directly selected for the secular equation is reduced and the weight of the reference configurations in the total CI expansion is correspondingly larger than in the VCI. It is also seen that there is hardly any difference (with the exception of the total MRD-CI space, of course) whether the virtual CH_3-LMO are included in the CI or not.

On the other hand, it is clear that the 10-electron LCI is not able to describe the $CH_3N_2^+$ dissociation correctly (Table 2); such calculation reproduces essentially the uncorrelated SCF value for the bond-breaking energy. Since the bond-breaking involves a considerable charge transfer from CH_3 to N_2, the inclusion of the correlation in the CH_3 bonds is also required for an adequate treatment of the entire process.

The conclusions from this sections are:

(1) Localized MO seem to give a more compact CI expansion than canonical MO, provided the system has a certain size (larger than the separated fragments N_2 or CH_3). This is due to the fact that excitations from the LMO occur predominantly in such virtual orbitals which are localized in the same region of space. In the example discussed it is best seen from the finding that the excitations from orbitals localized in the N_2 region into the virtual orbitals corresponding to the CH bonds, which are in principle possible (about 30,000 in the total MRD-CI space, Table 1), are not among those contributing to the total energy (i.e. less than 50 are among those SAF actually selected). This is consistent with the finding of Pulay et al. [24–26] who designed a "local correlation" procedure in which only such excitations are considered which are in the same local region as the electrons in the ground state configuration.

(2) The "local active region", which is described by correlated wavefunctions, must be large enough; in charge-transfer processes a correlated treatment of both partners is essential.

4. Calculations on the ethyldiazonium ion $CH_3CH_2N_2^+$

The optimized geometry of $CH_3CH_2N_2^+$ is displayed in Fig. 3. Identical CH distances and the HCC angles have thereby been assumed in the methyl group. Furthermore, the CNN angle was chosen to be 180°, since Ford [22] has obtained an angle of 179.6° in a full optimization of the system on the HF/6-31G* level. In comparison with $CH_3N_2^+$ the NN distance is basically the same, while the CN bond is longer by 7 pm indicating a weaker bond than in $CH_3N_2^+$.

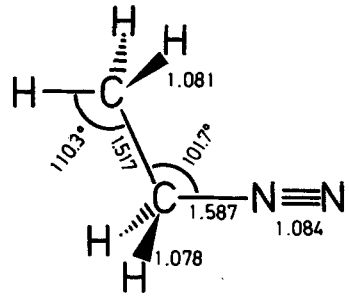

Fig. 3. Calculated equilibrium structure of $CH_3CH_2N_2^+$ (bond lengths in Å)

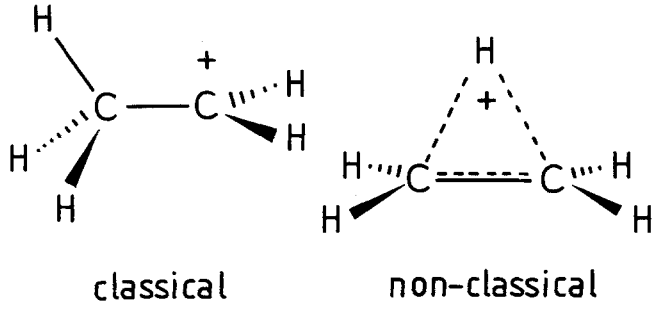

Fig. 4. Possible structures of the ethyl cation

Even though the ethylcation [27–29] possesses a non-classical structure (Fig. 4) the classical $C_2H_5^+$ structure has been chosen for the present studies, since the main goal was to see to what extent the CH_3 group, now separated from the N_2 by the CH_2 group, can be treated outside of the "local active region" of the molecule. At the SCF level the classical structure is stable. In addition to single-point calculations also potential curves have been obtained for this system.

4.1. Equilibrium and separated fragments

In order to obtain a proper set of MO for the multi-reference CI calculations, the orbitals are optimized in a complete-active-space (CAS) SCF calculation [12]. The CAS consisted of the orbitals localized in the N_2 area in addition to the σ(CN) orbital, i.e. 10 electrons were correlated in 10 orbitals in this CASSCF procedure. In order to restrict the configurations in the CAS, however, excitations from σ-type MO's into π-type were excluded, so that six electrons in six σ-type MO and four electrons in π-type MO were correlated in the CASSCF treatment. This procedure lead to a total of 3458 SAF for orbital optimization, and a CASSCF dissociation energy for $CH_3CH_2N_2^+ \rightarrow CH_3CH_2 + N_2$ of 0.61 eV compared to the value of 0.42 eV from a simple SCF procedure.

The CASSCF optimized doubly-occupied and virtual orbitals were then localized in the standard manner according to the Boys-localization procedure [15]. This localization turned out to be straightforward, because the CAS-active orbitals were automatically localized around the N_2 framework, i.e. representing a nitrogen lone pair, the triple bond and the σ(CN) bond. The CAS-inactive orbitals were transformed into the σ(CC) and the two σ(CH) bonds of the central carbon plus the three CH bonds of the terminal CH_3 frame.

In the valence CI (VCI) calculation 22 electrons were correlated; in the LCI only 16 electrons were correlated since the three electron pairs of the CH bonds in the methyl group were not included in the CI according to the division into local active region and spectator region. So the active region consisted of the orbitals corresponding to the NN, CN, CC and central CH bonds plus the nitrogen lone pair and the respective virtual counterparts. Because of the large number of correlated electrons in the VCI calculations additional CI calculations employing the MCPF procedure [12, 30] were also undertaken in order to study size-consistency effects.

The VCI are undertaken with one and with 16 reference configurations and are denoted by VCI(1) and VCI(16) (Table 3). The contribution of the dominant

Table 3. $CH_3CH_2N_2^+$: Influence of the orbital basis on the convergence of the CI expansion

Method	$E(T)$	$E_{\text{MRD-CI}}$	$E_{\text{est.FCI}}$	$\Sigma^{\text{Ref}} c_i^2$	SAF total	SAF selected	Energy sum
			$CH_3CH_2N_2^+$				
VCI(1)[a]/SCF MO	−0.74101	−0.78944	−0.85444	0.870	81091	18182	0.06746
VCI(1)[a]/SCF LMO	−0.76833	−0.78738	−0.85215	0.870	81091	6319	0.02165
VCI(1)/SCF LMO	−0.77821	−0.78841	−0.85448	0.867	81091	9665	0.01095
VCI(1)[b]	−0.79066	−0.79066	−0.85922	0.862	81091	81091	0.00000
LCI(1)[a]/SCF LMO	−0.66684	−0.67968	−0.72195	0.889	43215	4482	0.01346
LCI(1)/SCF LMO	−0.67404	−0.68091	−0.72412	0.889	43215	6629	0.00663
LCI(1)[b]	−0.68316	−0.68316	−0.72823	0.885	43215	43215	0.00000
VCI(16)/CAS MO	−0.78364	−0.81514	−0.85497	0.899	4154410	19093	0.03566
VCI(16)/CAS LMO	−0.79479	−0.81910	−0.86005	0.897	4154410	11182	0.02299
LCI(16)/CAS LMO	−0.69082	−0.70776	−0.72994	0.922	1981617	7751	0.01467
LCI(16)[c]/CAS LMO	−0.68414	−0.69934	−0.72043	0.924	1198019	7193	0.01300
			$CH_3CH_2^+ + N_2$				
VCI(1)[a]/SCF MO	−0.75453	−0.75899	−0.82423	0.865	81091	5701	0.00595
VCI(1)[a]/SCF LMO	−0.75075	−0.75778	−0.82171	0.868	81091	4699	0.00633
VCI(1)/SCF LMO	−0.75534	−0.75809	−0.82277	0.866	81091	5904	0.00240
VCI(1)[b]	−0.75928	−0.75928	−0.82499	0.864	81091	81091	0.00000
LCI(1)[a]/SCF LMO	−0.64075	−0.64430	−0.68404	0.891	43215	2777	0.00242
LCI(1)/SCF LMO	−0.64327	−0.64452	−0.68466	0.891	43215	3273	0.00081
LCI(1)[b]	−0.64545	−0.64545	−0.68613	0.890	43215	43215	0.00000
VCI(16)/CAS MO	−0.77264	−0.78743	−0.82821	0.894	4154410	8769	0.01257
VCI(16)/CAS LMO	−0.77339	−0.78968	−0.83055	0.895	4154410	7040	0.01131
LCI(16)/CAS LMO	−0.66059	−0.67199	−0.69255	0.924	1981617	4116	0.00648
LCI(16)[c]/CAS LMO	−0.65375	−0.66456	−0.68410	0.926	1198019	3705	0.00591

SCF energy of $CH_3CH_2N_2^+$: −187.29089 a.u.
CASSCF energy of $CH_3CH_2N_2^+$: −187.46187 a.u.
SCF energy of $CH_3CH_2^+ + N_2$: −187.27530 a.u.
CASSCF energy of $CH_3CH_2^+ + N_2$: −187.43954 a.u.
VCI(n) = valence CI with n Mains (22 electrons correlated)
LCI(n) = "local active region" CI with n Mains (16 electrons correlated)
Energies in a.u.; $E(T)$, $E_{\text{MRD-CI}}$ and $E_{\text{est.FCI}}$ relative to −187 a.u.
Selection threshold $T = 2\ \mu$H unless otherwise specified
[a] Selection threshold $T = 5\ \mu$H
[b] Selection threshold $T = 0$
[c] Virtual CH_3-LMO not included in the CI

configuration to the single-reference CI expansion is only about 87%; 16 reference configurations make approximately 90% of the total CI, based on their combined c^2 value (Table 3). The reference set was chosen in the following manner: all configurations which contributed more than $c^2 = 0.0025$ to the CAS wavefunction at equilibrium or in the separated fragments, plus the configurations $10a'^2(\sigma_{NN}) \rightarrow 14a'^2(\sigma^*_{NN}, \sigma^*_{CN})$, and $11a'^2(\sigma_{NN}, \sigma_{CN}) \rightarrow 15a'^2(\sigma^*_{NN}, \sigma^*_{CN})$ relative to the SCF ground state in the notation $1a'^2 \ldots 12a'^2, 1a^{*2} \ldots 3a^{*2}$; the latter two double substitutions were chosen because various $10a' \rightarrow 14a'$ and $11a' \rightarrow 15a'$ configurations appeared among the former set. As expected, the contribution of the SCF configuration to the total CI expansion was reduced to $c^2 = 0.85$ when 16 reference species were chosen; the next important configurations resulted, just as in $CH_3N_2^+$, from $\pi_{NN} \rightarrow \pi^*_{NN}$ type excitations with $c^2 = 0.01$.

If we turn now to the convergence pattern of the CI expansion by employing different molecular basis functions we observe the following:

At the equilibrium structure the estimated full CI energy is within 0.008 a.u. the same regardless of whether SCF MO, LMO, CAS MO or a single-reference treatment with threshold $T = 0$ is employed in the VCI calculations. As expected, there are variations between the various treatments, and the energy estimates derived from the procedure employing 16 reference configurations are also somewhat different from those employing only a single determinant in the SD-CI procedure. If the other quantities of Table 3 are compared it is also obvious that the LMO lead to a more rapid convergence in the VCI calculations: the $E(T)$ is considerably lower for the VCI(1)/LMO compared to VCI(1)/SCF MO whereby the computational expenditure is considerably reduced, because the number of selected SAF is only one third of that obtained for the same selection threshold employing SCF MO. The contribution of the unselected configurations is only about one third if the VCI/LMO is considered relative to VCI/SCF MO. These observations are carried over to the multi-reference treatment employing CAS MO; the number of selected configurations employing LMO is, for example, only half of that using CAS MO in the VCI(16) treatment.

For the separated fragments the convergence pattern is not as enhanced: for the VCI calculations with one reference configurations only, the canonical SCF MO and the LMO show a comparable truncated CI expansion length which is also found in the multi-reference case comparing CAS LMO and canonical orbitals (CAS MO).

A closer look at the calculated dissociation energies (Table 4) makes the more compact CI expansion by employing LMO again visible from a different point of view: The dissociation energy obtained in the single-reference VCI calculation at configuration selection threshold of $T = 5\ \mu H$ (corresponding to 18182 SAF out of a total of 81091 at equilibrium) gives a negative dissociation energy, and only the perturbation-like treatment to include the entire MRD-CI space leads to the value of 0.83 eV comparable with the results of all the other treatments. There is also little difference between the values obtained at the MRD-CI level and those employing the Davidson correction for the full CI estimate. The difference between the $\Delta E(T)$ values and those of the entire MRD-CI space $\Delta E_{MRD\text{-}CI}$ is much smaller if LMO are employed; it is also obvious, that the treatments should employ selection thresholds smaller than $5\ \mu H$, which is easily possible for LMO but more difficult for the calculations employing SCF MO.

In summary it can be stated that LMO yield a more compact CI expansion than canonical (SCF or CASSCF) orbitals, in particular for the molecule. The

Table 4. Dissociation energy of $CH_3CH_2N_2^+$

Method	$\Delta E(T)$ (eV)	$\Delta E_{\text{MRD-CI}}$ (eV)	$\Delta E_{\text{est.FCI}}$ (eV)
VCI(16)[a]/CAS LMO	0.30	0.75	0.73
VCI(16)/CAS LMO	0.58	0.80	0.80
VCI(1)[a]/SCF MO	−0.37	0.83	0.82
VCI(1)[a]/SCF LMO	0.48	0.82	0.83
VCI(1)/SCF LMO	0.62	0.83	0.86
VCI(1)[b]	0.85	0.85	0.93
VMCPF/SCF LMO			0.94
LCI(16)/CAS LMO	0.82	0.95	1.02
LCI(16)[c]/CAS LMO	0.83	0.95	0.99
LCI(1)[a]/SCF LMO	0.71	0.96	1.03
LCI(1)/SCF LMO	0.84	0.99	1.07
LCI(1)[b]	1.03	1.03	1.15
LMCPF/SCF LMO			1.19

The SCF value is 0.42 eV, the CASSCF value is 0.61 eV
VCI(n) = valence CI with n Mains (22 electrons correlated)
LCI(n) = "local active region" CI with n Mains (16 electrons correlated)
Selection threshold $T = 2\ \mu$H unless otherwise specified
[a] Selection threshold $T = 5\ \mu$H
[b] Selection threshold $T = 0$
[c] Virtual CH_3-LMO not included in the CI

fragments are relatively small entities so that the advantage of LMO versus canonical MO is only minor. A closer look at the calculated energies in the molecule and the separated fragments shows that the description of the correlation energy of the triple N_2 bond is somewhat more difficult for LMO than for the canonical MO. The best approach would be to treat the N_2 triple bond with CAS MO and the remaining molecular part by employing LMO. In what follows we want to compare VCI with LCI expansions. Since only 16 electrons are correlated the total energies (Table 3) are higher than in the VCI treatments which correlate 22 electrons. Likewise all total MRD-CI spaces are smaller, i.e. only 50% or less in the LCI(1) and LCI(16) treatments for both nuclear conformations, i.e. molecule and separated fragments. Accordingly the selected subspaces are also smaller and the entire calculation more efficient. The convergence pattern employing a series of thresholds $T = 5\ \mu$H, $T = 2\ \mu$H and $T = 0$ is consistent in the LCI(1) and LCI(16) calculations at all three levels $E(T)$, $E_{\text{MRD-CI}}$ and the error in the extrapolated $E_{\text{MRD-CI}}$ energy by employing 6629 SAF instead of the actual 43215 is only 0.0022 a.u. in the LCI(1) for the equilibrium structure, and less (i.e. 0.0009 a.u.) for the separated fragments, based on the 3273 instead of the 43215 SAF (Table 3).

The calculated dissociation energies (Table 4) show similar values as the VCI treatments. In particular the E_{MRDCI} values are very consistent between 0.95 eV and 1.03 eV. All values obtained from the estimated full LCI are higher by about 0.15–0.2 eV than those of corresponding VCI, however. Furthermore, it is seen that for the dissociation energy it is immaterial whether the virtual orbitals of the CH_3 groups are partially occupied by the 16 electrons in the CI or not: The dissociation energy is 0.95 eV in both cases ($E_{\text{MRD-CI}}$ value) and the only real

difference is that the MRD-CI space is 1981617 by considering the virtuals and roughly 800000 SAF less (1198019) if these orbitals are excluded from consideration.

The source for the difference of 0.15–0.2 eV between the VCI and LCI values for the dissociation energy is not entirely clear. Differences between VCI(16)/CAS LMO and LCI(16)/CAS LMO are very similar to those obtained from VCI(1)/SCF LMO and LCI(1)/SCF LMO so that the effect of the multi-reference treatment is similar in both types VCI or LCI calculations. The simpler (and cheaper) single-reference calculations can serve to study what effect (a) configuration selection and (b) size-consistency has on the calculated dissociation energy in the VCI and LCI treatment: (a) the pattern for the $\Delta E_{\text{MRD-CI}}$ as a function of selection threshold (5 μH, 2 μH, 0.0 μH) is parallel in the VCI(1) and LCI(1) calculations, so that the extrapolation to zero-threshold is valid also for the LCI variant. (b) The size-consistency error has a small influence, if one compares the value for the dissociation energy obtained at the rest. FCI level of VCI(1) at the threshold $T = 0$ with the VMCPF value on one side and the values form LCI(1) with those of LMCPF at $T = 0$ on the other [12]. So the difference between the correlation of all valence electrons and the correlation of only the electrons of the local active region is not affected by the (nearly) size-consistent MCPF treatment. Summarizing, we find that the deviation between the VCI and the LCI result is neither an artefact of the selection procedure nor of size-consistency effects.

Since all VCI calculations are carried out with 22 electrons and the LCI computations with only 16 electrons there is the question whether the difference is due to the correlation energy of the CH_3 group not taken into account in the LCI. For this reason the correlation energy between the CH_3 (as part of C_2H_6) and CH_3^+ (as part of $C_2H_5^+$) has been studied; after all in the molecule $CH_3CH_2N_2^+$ the CH_3 framework is neutral to a large extent while in the separated products $CH_3CH_2^+ + N_2$ there is a definite trend towards a more positive CH_3 surrounding. The results are listed in Table 5. It is seen that the local correlation energy for CH_3 is larger by 0.3 eV in the ethylcation than in ethane itself. It is thus quite probable that the difference in the dissociation energy from the LCI and VCI treatment is due to a difference in the CH_3 correlation energy of fragments and $CH_3CH_2N_2^+$ molecule.

Table 5. Correlation energy of the methyl group in C_2H_6 and $C_2H_5^+$ (energies in eV)

Method	C_2H_6			$C_2H_5^+$			
	$E_{\text{corr}}^{\text{VCI}}$	$E_{\text{corr}}^{\text{LCI}}$	$E_{\text{corr}}^{\text{CH}_3}$	$E_{\text{corr}}^{\text{VCI}}$	$E_{\text{corr}}^{\text{LCI}}$	$E_{\text{corr}}^{\text{CH}_3}$	$\Delta E_{\text{corr}}^{\text{CH}_3}$
CI(1)[a]/SCF LMO	7.38	4.09	3.29	6.49	2.86	3.63	0.34
CI(1)[b]	7.41	4.12	3.29	6.52	2.88	3.64	0.35
MCPF/SCF LMO	8.12	4.31	3.81	7.09	2.96	4.13	0.32

$E_{\text{corr}}^{\text{CH}_3} = E_{\text{corr}}^{\text{VCI}} - E_{\text{corr}}^{\text{LCI}}$

VCI(n) = valence CI with n Mains (14 electrons correlated in C_2H_6 and 12 correlated in $C_2H_5^+$)

LCI(n) = "local active region" CI with n Mains (8 electrons correlated in C_2H_6 and 6 correlated in $C_2H_5^+$)

[a] Selection threshold $T = 5$ μH

[b] Selection threshold $T = 0$

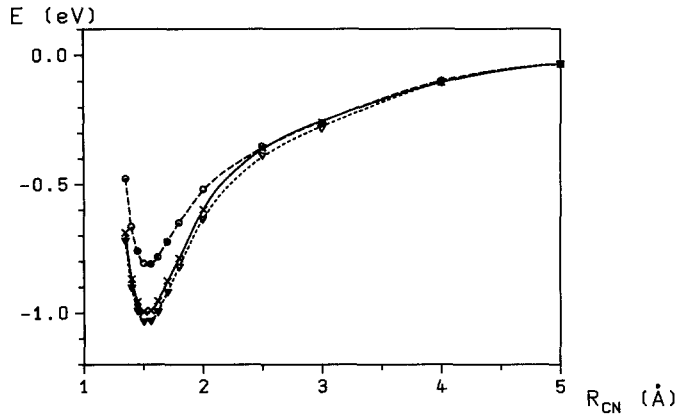

Fig. 5. Potential curves for $CH_3CH_2N_2^+$. ○ VCI(16)/CAS LMO. × LCI(16)/CAS LMO (virt. CH_3-LMO not in CI). ▽ LCI(16)/CAS LMO (virt. CH_3-LMO in CI)

4.2. Calculated potential energy curves

In order to see how the various methods perform over a larger range of geometrical variations, the potential curve for the C–N separation was calculated. Three different procedures were employed: (1) a valence CI with 16 reference configurations (22 electrons correlated) on the basis of localized orbitals, referred to as VCI(16)/CAS LMO, (2) the CI for the local active region consisting of the orbitals corresponding to NN, CN, CC and central CH bonds plus nitrogen lone pair and their virtual counterparts, correlating 16 electrons, referred to as LCI(16)/CAS LMO, in which again 16 reference configurations are chosen and finally (3) the equivalent LCI(16)/CAS LMO in which occupation of the virtual LMO in the CH_3 region are also allowed variable occupation. The calculated curves are displayed in Fig. 5.

Various observations can be made: First, the curve which corresponds to the LCI calculation in which the virtual CH_3-LMO are also included in the CI is slightly below the standard LCI curve; both are essentially parallel, however. The lower dissociation energy of about 0.2 eV from the LCI curve relative to that of the VCI treatment has already been discussed in the preceding section. Secondly, the optimum CN bond length (Table 6) is the same within 1 pm in the three calculations. It is shorter by 6 pm than in the SCF treatment. Hence it is clear that electron correlation is important in the description of the system, whereby

Table 6. $C_2H_5N_2^+$: potential curve parameters

Method	E_{diss}(eV)	R_{CN}(Å)	Curvature (hartree/bohr^2)
VCI(16)/CAS LMO	0.81	1.534	0.115
LCI(16)/CAS LMO	1.04	1.524	0.130
LCI(16)[a]/CAS LMO	1.00	1.521	0.131

VCI(n) = valence CI with n Mains (22 electrons correlated)
LCI(n) = "local active region" CI with n Mains (16 electrons correlated)
Selection threshold $T = 2\,\mu$H
[a] Virtual CH_3-LMO not included in the CI

LCI treatments reproduce VCI calculations very satisfactorily. And finally, the curvature of the VCI curve is reproduced to within 10% by the LCI procedure.

In summary then the conclusion from the first section, namely that the localized orbitals allow for a more compact and thus less expensive CI expansion is supported. Since the CH_3 group is not a direct neighbor of the bond-breaking area, i.e. the local active region has been enlarged to include the CH_2–N_2 area, it is found that the LCI reproduces the entire potential curve obtained in the standard VCI procedure with respect to shape and energetic location very satisfactorily.

5. Calculations for the dissociation of radicals

The LCI approach has also been employed for a number of simple reactions of the type CH_3–X and CH_3CH_2–X whereby X has different polarity; X = H can be characterized as non-polar, X = F as polar (electronegative) and $X = NH_3^+$ as strongly polar (positive). The calculated dissociation energies are listed in Table 7 and are compared with corresponding values obtained from an SCF calculation and a VCI treatment. All CI calculations employ only a single reference configuration; localized orbitals derived from the SCF canonical orbitals are employed as molecular orbital basis, and the same configuration selection threshold of $T = 5\,\mu H$ is used throughout. For the fragments (taken as a supermolecule) SCF calculations for the lowest triplet state have been performed in order to obtain the canonical orbitals as input for the localization procedure. Technical details of the various CI calculations and total energies obtained are summarized in Tables 8 and 9. Table 7 lists also the data for $CH_3N_2^+$ and $CH_3CH_2N_2^+$ in the respective treatments. In addition the bond-breaking of R–X with $X = NH_3^+$ is also investigated when a charge transfer takes place so that the fragment is NH_3 rather than NH_3^+.

Table 7. Dissociation energies of some radical reactions and charge transfer reactions

Reaction	SCF	LCI	VCI	SCF-VCI	LCI-VCI
CH_3–H → $CH_3\cdot + \cdot H$	4.05	4.70[a]	4.63	−0.58	0.07
CH_3CH_2–H → $CH_3CH_2\cdot + \cdot H$	4.01	4.76	4.70	−0.69	0.06
CH_3–F → $CH_3\cdot + \cdot F$	3.11	4.43	4.30	−1.19	0.13
CH_3CH_2–F → $CH_3CH_2\cdot + \cdot F$	3.31	4.58	4.49	−1.18	0.09
CH_3–NH_3^+ → $CH_3\cdot + \cdot NH_3^+$	3.99	4.89	4.94	−0.95	−0.05
CH_3CH_2–NH_3^+ → $CH_3CH_2\cdot + \cdot NH_3^+$	4.18	5.33	5.34	−1.16	−0.01
CH_3–NH_3^+ → $CH_3^+ + NH_3$	4.14	4.20	4.84	−0.70	−0.64
CH_3CH_2–NH_3^+ → $CH_3CH_2^+ + NH_3$	3.17	4.01	3.76	−0.59	0.25
CH_3–N_2^+ → $CH_3^+ + N_2$	1.22	1.15	1.73	−0.51	−0.58
CH_3CH_2–N_2^+ → $CH_3CH_2^+ + N_2$	0.42	1.03	0.83	−0.41	0.20

Energies in eV, the CI-energies are given on est. FCI level

[a] The extrapolation formula proposed by Pople et al. [31] gives 4.69 eV

All calculations are 1 Main CI calculations with SCV LMO

For the radical fragments triplet-SCF calculations were performed

Selection threshold $T = 5\,\mu H$

Table 8. VCI data of some radical reactions and charge transfer reactions

Species	$E_{MRD\text{-}CI}$	$E_{est.FCI}$	c^2	SAF total	SAF selected	Energy sum
CH_3–H	−40.34843	−40.35685	0.944	1441	941	0.00082
$CH_3\cdot + \cdot H$	−40.17968	−40.18658	0.947	2841	942	0.00070
CH_3CH_2–H	−79.50475	−79.52900	0.911	13972	3348	0.00786
$CH_3CH_2\cdot + \cdot H$	−79.33531	−79.35636	0.916	30852	4636	0.01353
CH_3–F	−139.36873	−139.39005	0.929	9409	2376	0.00572
$CH_3\cdot + \cdot F$	−139.21399	−139.23201	0.931	20638	1609	0.00123
CH_3CH_2–F	−178.52717	−178.56853	0.898	45577	4957	0.01555
$CH_3CH_2\cdot + \cdot F$	−178.36732	−178.40441	0.902	104536	4847	0.01274
CH_3–NH_3^+	−95.88062	−95.90584	0.914	13972	3044	0.00775
$CH_3\cdot + \cdot NH_3^+$	−95.70212	−95.72424	0.916	30852	2056	0.00165
$CH_3^+ + NH_3$	−95.70536	−95.72815	0.916	13972	1393	0.00070
CH_3CH_2–NH_3^+	−135.03977	−135.08542	0.888	59413	5015	0.01795
$CH_3CH_2\cdot + \cdot NH_3^+$	−134.84897	−134.88924	0.892	136633	5321	0.01361
$CH_3CH_2^+ + NH_3$	−134.90343	−134.94739	0.887	59413	3710	0.00597

Energies in a.u.
All calculations are 1 Main CI calculations with SCF LMO
For the radical fragments triplet-SCF calculations were performed
Selection threshold $T = 5\ \mu H$

Table 9. LCI data of some radical reactions and charge transfer reactions

Species	E_{MRDCI}	$E_{est.FCI}$	c^2	SAF total	SAF selected	Energy sum
CH_3–H	−40.22174	−40.22199	0.990	120	63	0.00009
$CH_3\cdot + \cdot H$[a]						
CH_3CH_2–H	−79.31291	−79.39119	0.945	4671	1569	0.00268
$CH_3CH_2\cdot + \cdot H$	−79.21036	−79.21639	0.952	9491	1822	0.00371
CH_3–F	−139.25717	−139.26425	0.963	3157	1063	0.00157
$CH_3\cdot + \cdot F$	−139.09735	−139.10150	0.971	6363	621	0.00032
CH_3CH_2–F	−178.41280	−178.43468	0.928	22504	3222	0.00904
$CH_3CH_2\cdot + \cdot F$	−178.24890	−178.26649	0.932	50013	2251	0.00367
CH_3–NH_3^+	−95.76258	−95.77174	0.948	4671	1509	0.00241
$CH_3\cdot + \cdot NH_3^+$	−95.58521	−95.59200	0.953	9491	1060	0.00073
$CH_3^+ + NH_3$	−95.60797	−95.61730	0.946	4671	883	0.00044
CH_3CH_2–NH_3^+	−134.92637	−134.95132	0.915	29317	3290	0.01046
$CH_3CH_2\cdot + \cdot NH_3^+$	−134.73463	−134.75542	0.919	65347	2841	0.00433
$CH_3CH_2^+ + NH_3$	−134.78222	−134.80405	0.918	29317	1760	0.00179

Energies in a.u.
All calculations are 1 Main CI calculations with SCF LMO
For the radical fragments triplet-SCF calculations were performed
Selection threshold $T = 5\ \mu H$
[a] In this 'LCI' no electrons were correlated. The SCF energy is −40.04939 a.u.

It is obvious from Table 7 that the SCF values exhibit large errors, as expected. It is furthermore seen that the LCI reproduces the dissociation energies relative to the VCI values within approximately 0.1 eV. This is fairly independent of the polarity of the group, although a minor trend (LCI-VCI value larger for the negative and smaller for the positive fragment relative to the non-polar hydrogen) can be made out. For the longer chain CH_3CH_2–X the difference between the LCI and VCI values are even smaller than if cleavage takes place next to the CH_3 group.

From a technical point of view it is also obvious (Tables 8, 9) that the amount of computer time needed is much smaller for the LCI treatment; for CH_3CH_2–H, for example, the total and selected number of SAF in the VCI treatment are 13972 (3348) and 30852 (4636) for the molecule and the fragments, respectively, with the number of selected SAF given in parentheses, while the corresponding numbers in the LCI are only 4671 (1569) and 9491 (1822), i.e. a reduction in the size of the configuration space by a factor of roughly three.

In contrast to the dissociation into radicals, in which the bond-breaking is a fairly local process, the bond-breaking accompanied by a charge transfer affects a larger portion of the molecule. If the local active region is restricted to the immediate neighborhood of the dissociating group, as done for the last two examples in Table 7, considerable errors occur in the LCI treatment, as has been discussed in the earlier sections. The situation for the NH_3 dissociation (rather than the NH_3^+) from R is thereby wholly analogous to that in $CH_3N_2^+$ and $CH_2CH_3N_2^+$: The dissociation energy is drastically underestimated in the LCI for $CH_3NH_3^+$ if the CH_3 bonds are not included in the lcoal active region, and it is slightly overestimated in the longer chain.

6. Summary and conclusion

Three points emerge from the various calculations carried out in the present work.

(1) The use of localized orbitals instead of canonical orbitals leads to a more compact CI expansion in molecular calculations.

(2) If the bond-breaking can be considered a fairly local process, as in the dissociation of the various radicals studied, the molecule can be divided into a "local active region" and a "spectator group"; it seems sufficient to treat the former part by elaborate methods which account for electron correlation, i.e. by a local CI, while the electrons in the spectator group can be left uncorrelated. It is found that the dissociation energies for R–X separation (X = H, F, NH_3^+ and R = CH_3 or CH_3CH_2) obtained by considering CH_3 as the spectator differ by less than 0.1 eV from the value obtained by employing a CI for the entire molecule. This approach, based on a CI with localized orbitals, reduces the computational expenditure considerably. If charge transfer takes place during bond-breaking a larger part than the immediate neighborhood of the bond cleavage is affected and the "local active region" may spread over a larger portion of the molecule.

(3) The virtual orbitals of the "spectator group" can also be deleted from the local CI without loss of accuracy.

These findings suggest to employ localized orbitals and local CI for the treatment of larger molecules. It will be interesting to see whether electronic

excitations attributed to certain chromophores can also be investigated by the same kind of approach of a local active region and a spectator group. Finally, it is conceivable to simply replace the spectator group by an appropriate effective potential if the electron correlation of the spectator has no influence on the process of interest. Further work on this aspect is under way.

Acknowledgements. The authors thank Dr. Christel Marian for various helpful discussions and advice in using the CASSCF program package made available to us by the Stockholm group. The financial support of the DFG is gratefully acknowledged. The calculations have been carried out on the CONVEX C220 of the SFB 334.

References

1. Shavitt I (1977) in: Schaefer III HF (ed) Modern theoretical chemistry, Vol 3: Methods of electronic structure theory 198. Plenum Press, NY
2. Barr TL, Davidson ER (1970) Phys Rev A 1:64
3. Buenker RJ, Peyerimhoff SD (1974) Theor Chim Acta 35:33
4. Thunemann KH, Römelt J, Peyerimhoff SD, Buenker RJ (1977) Int J Quantum Chem 11:743
5. Bender CF, Davidson ER (1966) J Chem Phys 70:2675
6. Roos BO, Taylor PR, Siegbahn PEM (1980) Chem Phys 48:157
7. Kaufmann JJ, Hariharan PC, Roszak S, van Hemert M (1987) J Comp Chem 8:736
8. Kaufmann JJ, Hariharan PC, Keegstra PB (1987) Int J Quantum Chem, Quantum Chem Symp 21:623
9. Roszak S, Keegstra PB, Hariharan PC, Kaufmann JJ (1988) Int J Quantum Chem, Quantum Chem Symp 22:619
10. Roszak S, Keegstra PB, Hariharan PC, Kaufmann JJ (1989) Int J Quantum Chem 36:353
11. Dunning Jr TH (1970) J Chem Phys 53:2823
12. The SDCI and MCPF program (for single reference calculations with threshold = 0) and the CASSCF program are part of the SWEDEN package of Siegbahn PEM, Bauschlicher Jr. CW, Roos B, Taylor PR, Heilberg A, Almlöf J, Langhoff SR, Chong DP
13. Bonifacic V, Huzinaga S (1974) J Chem Phys 60:2779
14. Durand P, Barthelat JC (1975) Theor Chim Acta 38:283
15. Foster JM, Boys SF (1960) Rev Mod Phys 32:300
16. Buenker RJ, Peyerimhoff SD, Butscher W (1978) Mol Phys 35:771
17. Buenker RJ, Peyerimhoff SD (1975) Theor Chim Acta 39:217
18. Buenker RJ, Peyerimhoff SD, Bruna PJ (1981) in: Csizmadia IG, Daudel R (eds) Computational theoretical organic chemistry 55. D Reidel, Publ, Dordrecht, Holland
19. GAUSSIAN86 program package: Frisch MJ, Binkley JS, Schlegel HB, Raghavachari K, Melius CF, Martin RL, Steward JJP, Bobrowitcz FW, Rohlfing CM, Kahn LR, Defrees DJ, Seeger R, Whiteside RA, Fox DJ, Fleuder EM, Pople JA, Carnegie-Mellon Quantum Chemistry Publ Unit, Pittsburgh PA, 1984
20. Dewar MJS, Thiel W (1977) J Am Chem Soc 99:4899
21. Landolt-Börnstein, New Series, Vol. II/7, Structure Data of Free Polyatomic Molecules. Springer, Berlin, 1976
22. Ford GP (1986) J Am Chem Soc 108:5104
23. Vincent MA, Radom L (1978) J Am Chem Soc 100:3306
24. Saebo S, Pulay P (1985) Chem Phys Lett 113:13
25. Saebo S, Pulay P (1987) J Chem Phys 86:914
26. Saebo S, Pulay P (1988) J Chem Phys 88:1884
27. Raghavari K, Whiteside RA, Pople JA, v Schleyer P (l1981) J Am Chem Soc 103:5649
28. Hirao K, Yamabe S (1984) Chem Phys 89:237
29. Wong MW, Baker J, Nobes RH, Radom L (1987) J Am Chem Soc 109:2245
30. Chong DP, Langhoff SR (1986) J Chem Phys 84:5606
31. Pople JA, Seeger R, Krishnan R (1977) Int J Quantum Chem Symp 11:149